jove JOURNAL OF VISUALIZED EXPERIMENTS
1 Alewife Center #200
Cambridge, MA 02140
tel. 617.945.9051
www.jove.com

TITLE

Modeling stroke in mice: directed brain injury using photothrombotic model

AUTHORSANDAFFILIATIONS

Gemma Llovera[1] gemma.llovera-garcia@med.uni-muenchen.de
Kelsey Pinkham[1] kelsey.pinkham@med.uni-muenchen.de
Arthur Liesz[1,2] arthur.liesz@med.uni-muenchen.de

[1] Institute for Stroke and Dementia Research, LMU Munich, Feodor-Lynen-Strasse 17, 81377 Munich, Germany

[2] Munich Cluster for Systems Neurology (SyNergy), Munich, Germany

Corresponding Author:
Dr. Gemma Llovera
Institute for Stroke and Dementia Research,
LMU Munich,
Feodor-Lynen-Strasse 17
81377 Munich, Germany
phone: +49-89-4400-46182
email: Gemma.Llovera-Garcia@med.uni-muenchen.de

KEYWORDS:
stroke, brain ischemia, animal model, photothrombotic, permanent, Rose Bengal, laser illumination

SUMMARY:
Here, we describe the photothrombotic stroke model, where a stroke is produced through the intact skull by inducing permanent microvascular occlusion using laser illumination after administration of a photosensitive dye.

ABSTRACT:

Stroke is a leading cause of death and acquired adult disability in developed countries. Despite extensive investigation for novel therapeutic strategies, there remain limited therapeutic options for stroke patients. Therefore, more research is needed for pathophysiological pathways such as post-stroke inflammation, angiogenesis, neuronal plasticity and regeneration. Given the inability of in vitro models to reproduce the complexity of the brain, experimental stroke models are essential for the analysis and subsequent evaluation of novel drug targets for these mechanisms. To overcome the so-called "replication crisis", detailed standardized models for all procedures are urgently needed. As an effort within the "ImmunoStroke" research consortium (https://immunostroke.de/), we describe here astandardized photothrombotic mouse model using an intraperitoneal injection of Rose Bengal and the illumination of the intact skull with a 561nm laser. This model allows the performance of stroke in mice with allocation to any cortical region of the brain without invasive surgery. Thus, enabling the study of stroke in various areas of the brain. In this video, we demonstrate the surgical methods of stroke induction in the photothrombotic model as well as histological analysis.

INTRODUCTION:

Ischemic stroke remains a principal cause of death and acquired adult disability in developed countries in the 21st century. Accounting for approximately 2.7 million deaths in 2017 worldwide[1]. Even with the immense efforts of the scientific community, few treatments are available. Furthermore, with such high exclusion criteria, these already limited options are not accessible to many patients. Therefore, there is an urgent need for novel treatments to improve functional recovery after stroke.

Considering the incapability of *in vitro* models to replicate the complex interactions of the brain, animal models are essential for preclinical stroke research. Mice are the most frequently used animal model in the stroke research field. The majority of these mouse models aim to induce infarctions by blocking the blood flow within the middle cerebral artery (MCA) since the majority of human stroke lesions are located in the MCA territory[2]. Although these models very well reproduce human stroke lesions, involve complex surgeries and high infarct volume variability.

Since Rosenblum and El-Sabban's proposal of the photothrombotic model in 1977[3], and later Watson et *al.* application of this model to rats[4], it has become widely used in ischemic stroke research[5,6]. The photothrombotic stroke model induces a local and defined cortical infarct through the photo-activation of a light-sensitive dye previously delivered into the blood flow. This results in a local vessel thrombosis in the light-exposed areas. Briefly, when the circulating dye is illuminated at the appropriate wavelength, it releases energy to oxygen molecules, which in turn generates a large amount of highly reactive singlet oxygen products. These oxygen intermediates induce endothelial cell membrane peroxidation, leading to platelet adhesion, aggregation and eventually to the formation of thrombi which determine local cerebral

flow interruption[7].

The principal advantage of this technique resides in its simplicity of execution and the possibility to direct the lesion to the desired region. Unlike other experimental stroke models, minor surgical expertise is needed to perform the photothrombotic stroke model as the lesion is induced through simple illumination of the intact skull. Moreover, the well-delimited borders (**Figure 2A and 5B**) and the flexibility to induce the lesion to a specific brain region can facilitate the study of cellular responses within the ischemic or intact cortical area. For these reasons, this approach may be suitable forcellular and molecular studies of cortical plasticity.

Over the past few decades, the growing concern regarding the lack of reproducibility between research groups has been coined the so-called "replication crisis"[8]. After the coordination of the first preclinical randomized controlled multicenter trial study in 2015[9], a proposed tool to improve preclinical research[10-12], we confirmed that one cause for failing reproducibility between preclinical studies from independent laboratories was the lack of sufficient standardization of experimental stroke models and outcome parameters[13]. Accordingly, when the "ImmunoStroke" consortium was established (https://immunostroke.de/), which aims to understand brain-immune interactions underlying the mechanistic principles of stroke recovery, the standardization of all the experimental stroke models among each research group was essential.

Here, we describe the standardized procedure for the induction of the photothrombotic model as used in the above-mentioned research consortium. Briefly, an animal underwent anesthetics, received a Rose Bengal injection (10µL/g) intraperitonally, and immediately a 561nm laser illuminates the intact skull, 3mm left from bregma, for 20min (**Figure 1**). Additionally, we report a related histological and behavioral method to analyze the stroke outcome in this model. All methods are based on standard operating procedures developed and used in our laboratories.

PROTOCOL:

Ethics statement

The experiments reported in this video were conducted by national guidelines for the use of experimental animals, and the protocols were approved by the German governmental committees (Regierung von Oberbayern, Munich, Germany). We used 10-12 weeks old, male C57Bl/6J mice dispatched by Charles River Germany. The animals were housed under controlled temperature (22 °C ± 2 °C), with a 12h light-dark cycle period and access to pelleted food and water *ad libitum.*

1. Preparation of the material and instruments

1.1. Dissolve Rose Bengal in 0,9% saline solution to reach a final concentration of 10mg/ml and connect the heat blanket to maintain the operation area warm and maintain the mouse body temperature during anesthesia at 37 °C.

1.2. Prepare scissors, forceps, pieces of cotton, dexpanthenol eye ointment, and suture material. Prepare a syringe with saline solution (without needle) to maintain the operation area hydrated. Prepare the anesthesia gas (100% O_2 + isoflurane).

2. Preparation of the animal

2.1. Inject analgesia 30min before surgery (4 mg/kg Carprofen und 0.1 mg/kg Buprenorphine).

2.2. Record the mouse body weight to adjust the dose of Rose Bengal to be injected (10µL/g -100µg/g-).

2.3. Place the mouse into the induction chamber with an isoflurane flow rate of 4% to anesthetize it until the spontaneous movement of the body and vibrissae stops.

2.4. Transfer the mouse into the stereotactic frame and place it in a proneposition with its nose into the anesthesia mask, fix the animal and maintain isoflurane concentration at 4% for another minute, then reduce and maintain it at 2%.

2.5. Gently insert the rectal probe to monitor the temperature throughout the surgical procedures. Set the associated feedback-controlled heatingpad for maintaining the mouse body temperature at 37°C.

2.6. Apply dexpanthenol eye ointment to both eyes and clean the skin and surrounding fur with a disinfectant agent.

3. Photothrombosis model

3.1 Make a longitudinal incision 2.0-2.5 cm and retracted to expose the skull. To avoid wound complications the skull exposure should be achieved with a single cut.

3.2 Remove gently the periosteum with cotton and coronal sutures are identified.

3.3 Put on your protective glasses, switch on the 561nm laser and mark bregma +3mm left.

3.4 Switch off the laser, hook a sticker with a 4mm diameter hole placed at the marked coordinates mentioned above.

3.5 Inject the mouse with Bengal Rose (10µl/gr), intraperitoneally, place the laser beam at 4-5cm from the skull and switch on the 561nm laser and illuminate the skull for 20min.

3.6 Apply 2 drops of 0,9% saline to the skull to rehydrate, suture the wound and place the animal in a recovery chamber at 37°C to recover from anesthesia. After 1h returned mice to their cages in a temperature-controlled room.

3.7 Inject analgesia every 12h for 3d after surgery (4 mg/kg Carprofenand 0.1 mg/kg Buprenorphine).

4. Sham operation

Two different procedures of Sham operations are carried out. The first one: All procedures are performed identically to the operation described above, including the Rose Bengal injection without switching on the laser. After 20min under anesthesia, animals stay 1h in the recovery chamber to recover from anesthesia before being returned to their cages. The second one: All procedures are performed identically to the operation described above, without the Rose Bengal injection and switching on the laser. After 20min of laser illumination, animals stay 1h in the recovery chamber to recover from anesthesia before being returned to their cages.

5. Laser speckle

5.1. Connect the heat blanket to maintain the operation area warm and maintain the mouse body temperature during anesthesia at 37 °C.

5.2. Place the mouse into the induction chamber with an isoflurane flow rate of 4% to anesthetize it until the spontaneous movement of the body and vibrissae stops, then transfer the mouse into the stereotactic frame and place it in a prone position with its nose into the anesthesia mask, fix the animal and maintain isoflurane concentration at 4% for another minute, then reduce and maintain it at 2%.

5.3. Gently insert the rectal probe to monitor the temperature throughout the surgical procedures. Set the associated feedback-controlled heating pad for maintaining the mouse body temperature at 37 °C and apply dexpanthenol eye ointment to both eyes, clean the skin and surrounding fur with a disinfectant

agent and make a longitudinal incision 2.0-2.5 cm and retracted to expose the skull. To avoid wound complications the skull exposure should be achieved with a single cut.

5.4. Place the sterotactic frame under the laser speckle and adjust the height to obtain a sharp image and focus the laser speckle perfusion imaging (LSI) camera on the cranial window. Configure the high resolution laser speckle imaging (LSI) camera system as previously described[14]. Acquire data from a 1 cm x 1 cm field of view using a 785 nm wavelength and 80 mW lasers with a frame rate of 21 images/s at a working distance of 1 cm for 1 min.

5.5. After imaging, apply 2 drops of 0,9% saline to the skull to rehydrate, suture the wound and place the animal in a recovery chamber at 37 °C to recover from anesthesia for 1h. After 1h return mice to their cages in a temperature-controlled room.

6. Neuroscore

For the neurological deficit analysis, we used a modified neurological scale published by Eckenstein et al. in 1997 [15]. Briefly, animals are scored for general (**Table 1**) and focal deficits (**Table 2**). This composite scale ranges from 0 (no deficits) to 46 (severe impairments).

6.1. Perform the Neuroscore at the same time each day at the same time each day always at the same time of the dayand use surgical clothes to keep a “neutral smell”.

6.2. Habituate mice forHabituate mice for 30 min in the room with an “open” cage before the test and allow them to observe each item for 30s

7. Perfusion

7.1. Prepare a 20mL syringe containing PBS-heparin (2U/mL) and place it 1m above the bench to facilitate/ensure gravity-driven perfusion.

7.2. Inject intraperitoneally 100µL of ketamine and xylazine (120/16 mg/kg body weight, respectively). Wait 5min and corroborate cessation of spontaneous body movement and vibrissae.

7.3. Fix the animal in a supine position and disinfect the abdominal body surface with ethanol 100%. Make a 3-cm-long incision into the abdomen, cut the diaphragm and the ribs to completely visualize the heart.

7.4. Make a small incision in the right atrium and insert the perfusion cannula into the left ventricle and perfuse with 20mL PBS-heparin.

7.5. After perfusion, decapitate the animal and remove the brain, freeze it using dry ice and store them at -80°C until further use

8. Infarct volumetry

8.1 Cryosectioning: Cut the brains serially on a cryostat to 20 µm thick sections every 120 µm on slides. Store the slides at −80 °C until use.

8.2 Cresyl violet (CV) staining

8.2.1 Prepare the staining solution: Mix 0.5 g of CV acetate in 500 mL H_2O. Stir and heat (60 °C) until crystals are dissolved. Let the solution cool and store it in a dark bottle. Reheat to 60 °C and filter (paper filter) before every use.

8.2.2 Dry the slides at room temperature for 30 min. Then place them in 95% ethanol for 15 min, in 70% ethanol for 1 min, and afterward in 50% ethanol for 1 min.

8.2.3 Place the slides in distilled water for 2 min, refresh distilled water, and place them in again for 1 min. Afterward, place the slides in the pre-heated staining solution for 10 min at 60 °C. Wash the slides twice in distilled water for 1 min.

8.2.4 Place the slides in 95% ethanol for 2 min. Then place them into 100% ethanol for 5 min, refresh the 100% ethanol and place them in again for 2 min. Afterward, cover the slides with a mounting medium.

8.2.5 Analysis

Scan the slides and analyze the indirect infarct volume by the Swanson method[16] to correct for edema: (Ischemic area) = (ischemic region)-((ipsilateral hemisphere) – (contralateral hemisphere))

9. Tunel staining (ApopTag® Peroxidase In Situ Apoptosis Detection Kit)

9.1. Dry slides, post-fix in 4% PF in PBS (ph 7.4) for 10-20 min at RT, after wash in PBS, post-fix in precooled Ethanol: acetic acid 2:1 for 5 min at -20°C.

9.2. Wash in PBS and apply Equilibration Buffer (10s –max 60min- at RT) and apply Working Strength TdT Enzyme (1h at 37°C in humidified chamber)

9.3. Apply Working Strength STOP/WASH Enzyme (10min at RT), wash in PBS and apply warmed (RT) Working strength ANTI-DIGOXIGENIN CONJUGATE (30min at RT in dark)

9.4. Wash in PBS, incubate with DAPI 5min at RT and mount with fluoromount media.

REPRESENTATIVE RESULTS

The model that we described here is a photothrombotic stroke model by Rose Bengal injection and intact skull illumination for 20min, at constant 561 nm wavelength and 25 mW output power at the fiber. Although the complete photothrombotic surgery lasts 30min, the animal is kept under low anesthesia and the brain damage is moderate. Approximately 10 min after transfer to their cages all the animals were awake, freely moving in the cage and interacting with littermates.

We performed infarct volumetry using cresyl violet stained serial coronal brain sections 24h after stroke induction (**Figure 2A**). The mean infarct volume was 29.3 mm^3, representing 23% of one brain hemisphere. Moreover, the variability of this stroke model is exceptionally low with a standard deviation of approx. 3.5% (**Figure 2B**). The lesion area encompasses the motor cortex without the affection of subcortical structures.

Phototrombosis lesion caused a moderate, long term sensorimotor imparment, indicated by the composite Neuroscore[15] (**Figure 3**); general and focal deficits were measured 24h, 3d and 7d after surgery. The general Neuroscore has 5 items, including the evaluation of the fur, ears, eyes, posture and spontaneous activity, with a maximum score of 18 **(Table 1)**. The focal Neuroscore comprises 7 items, including the evaluation of body symmetry, gait, climbing, circling behavior, forelimb symmetry, compulsory cycling and whiskers response, with a maximum score of 28 **(Table 2)**. Stroke animals had a significant change in the composite neuroscore 24 hours after surgery compared to Sham-operated animals. These differences persisted, although stroke mice improved over time (**Figure 3).**

Mortality during the observation time after stroke induction occurs only very rarely in approx. 1-2% of animals. In the operation series of 10 animals for this report, all of the animals survived the operation and

during the 7d observation period, none of them had to be excluded due to exclusion criteria. We also monitored body weight and temperature changes in mice at 24 h, 3 and 7 days after surgery (**Figure 4A-B**). Data showed that body weight and temperature were decreased 24h after surgery only in the Rose Bengal+illumination group, but it recovers at 3 days after surgery at the level of the Sham-operated animals.

To confirm an induction of ischaemic changes, 24 hours after surgery, the animals underwent a laser imaging test. A laser speckle contrast imaging using the PeriCam PSI System (Peri-Cam PSI System, Perimed, Sweden) measured blood perfusion of the cortex during 1min and an averaged color coded picture was obtained for each animal. Showing that Rose Bengal or laser illumination alone do not produce a lesion, while simultaneous application of Rose Bengal and laser illumination generate a round hypoperfused area of 4mm diameter surrounded by a narrow oligemic zone **(Figure 5A).** In addition, a cresyl violet and Tunel staining for assessment of the infarct volume 24 hours after surgery revealed no tissue damage either in Rose Bengal or laser illumination surgeries. On the other hand, Rose Bengal+laser illumination generate a well-demarcated lesion **(Figure 5B)**.

FIGURE LEGENDS:

Table 1: General Neuroscore. For each of the five general deficits measured, animals can receive between 0 and 4 points depending on the severity. The scores on the five areas are then summed to provide a total general score ranging from 0-18.

Table 2: Focal Neuroscore. For each of the seven general deficits measured, animals can receive between 0 and 4 points depending on the severity. The scores on the five areas are then summed to provide a total general score ranging from 0-28.

Figure 1: Photothrombosis. Diagram depicting the photothrombotic area, 3mm from Bregma. The green dot indicates the position of the laser.

Figure 2: Volumetric infarct analysis and infarct outcome 24h after PT. A) Representative cresyl violet stained coronal brain, sections every 120 µm at 24h after PT. Dashed lines demarcate the lesion area. **B)** Infarct volume analysis of 10 brains (each dot representing one individual brain) 24h after PT. The horizontal red line represents the mean (29.32 mm^3), error bars indicate standard deviation (3.45 mm^3).

Figure 3: Neuroscore for functional deficits after PT. Composite Neuroscore before, 24h, 3d and 7d after PT. BL=before PT, RB=Rose Bengal. n=5 per group. *$p<0.05$.

Figure 4: Body weight and temperature analysis after PT. A) Body weight and **B)** temperature was slightly reduced in PT animals compare to Sham-operated groups at 24h and it recovered 3 days after PT.BL=before PT, RB=Rose Bengal.n=5 per group.*p<0.05.

Figure 5: Lesion confirmation after PT. A) Laser Speckle imaging **B)** Cresyl violet (upper panels) and Tunel staining (lower panels) confirmed the lesion only after administration of Rose Bengal and subsequent laser illumination. RB=Rose Bengal. Scale bar= 1000µm in upper panel B, scale bar= 20 µm in lower panel B.

DISCUSSION:

The presented protocol describes the experimental stroke model of photothrombosis by illuminating the intact skull with a 561nm laser, with a previous intraperitoneal injection of Rose Bengal. Until recently, the use of this model has been low but is steadily increasing.

Mortality during stroke induction in this model is absent. The overall mortality of less than 5% arises during operation due to anesthesiological complications or sacrifice after meeting the exclusion criteria. To warrant the low variability of this model and its reproducibility, we suggest the following exclusion criteria: 1) Operation time longer than 30 min 2) Infection of the suture 3) Bite wound 4) No infarct or no fore asymmetry at 24h after PT.

A widely used experimental stroke models being the transient occlusion of the MCA, by using a suture filament, which is introduced in the internal carotid artery until the silicon-coated tip occludes the origin of the MCA. This model allows the reperfusion by removing the filament and mimics the human clinical scenario, in which there is a restoration of the cerebral blood flow after spontaneous or therapeutic (rtPA) lysis of an embolic clot[17,18]. However, it involves a complex surgery with high variability of the final infarct and high mortality rate[9]. In contrast, the permanent occlusion of the MCA distal of the lenticulostriatal arteries can be achieved by coagulation of the artery[19,20], which induces locally defined lesions in the neocortex[21]. Although this model has a lower mortality rate, it requires invasive surgery to the animal by trepanation of the skull over the MCA to later coagulate it[22]. Consequently, high surgical skills are required for a successful and unbiased in vivo stroke study.

Compared to other brain ischemia models, the photothrombotic model as carried out in this video has the advantage of no craniotomy or major surgery on the animal. Unlike other models that involve complex surgeries or brain craniotomy. Moreover, the simple execution of the model makes the surgery accessible to many with low time-consuming training. Low mortality, moderate infarct volume, and flexibility to induce the lesion to a specific brain region, emphasize the advantage of this experimental paradigm for brain regeneration and stroke studies[23-26].

Despite the obvious advantages, a few limitations of this stroke model need to be taken into consideration. The long exposure of anesthetics to the animal might be a critical factor to take into account, as the impact of anesthetics on neuroprotection and stroke outcome is already well-known[27]. Although the duration of this surgical procedure takes approximately 30 minutes, the animal can be under low anesthetic concentrations due to the minimal manipulation of the animal during the 20 minutes of laser illumination. Because this model induces moderate brain injuries, only minor behavioral deficits are detectable. Thus, more advanced test systems with higher sensitivity and qualitative test parameters, such as the skilled reaching test[28] and Neuroscore[15], as described in here, maybe more suitable for detecting long-term functional outcomes in this model. Finally, due to the permanent aggregation of the platelets into the illuminated blood vessels, no reperfusion can be obtained, which is a feature observed in a substantial percentage of stroke patients due to spontaneous clot lysis or therapy[29].

A similar phototrombotic stroke model published on 2013 by Labat-gest and Tomasi, describing a PT protocol using a cold light lamp instead of a 561nm green laser[30]. Both laser and cold light sources can be used to induce Rose Bengal excitation. An advantage of laser-based light sources over cold light lamps is that lasers can be used to target individual surface arterioles for in-vivo vessel-specific clotting[31]. Although we were not aiming for targeting specific arterioles, we used a 561nm green laser for brain illuminationn and phototrombosis induction, because of Rose Bengal absortion peak at 562nm. To ensure a proper laser intensity during the illumination, we used the Cobolt Monitor™ Software-6.1.0.0 to calibrate the laser. Moreover, in the present study a Rose Bengal dosage of 10µl/g (100µl/g) was sufficient to induce phototrombosis, while the previous protocol reported a higher dosis (150µl/g)[30]. In addition we provide a behavioral method to analyze the stroke outcome (Neuroscore) and an additional sham-control group (laser illumination) in order to prove that the laser itself do not produce any tissue damage, so only the combination of RB+laser illumination induce a brain lesion.

Taken together, the non-invasive straight forward surgical procedure enables high reproducibility and directionality of the stroke lesion to the brain. Alongside the possibility of long-term observation due to minimal mortality, distinguish our photothrombotic stroke model as a valuable experimental paradigm for basic and translational stroke research.

ACKNOWLEDGMENTS

We thank all our collaboration partners of the Immunostroke Consortia (FOR 2879, From immune cells to stroke recovery) for suggestions and discussions. This work was funded by the Deutsche Forschungsgemeinschaft (DFG,German Research Foundation) under Germany's Excellence Strategy within the framework of the Munich Cluster for Systems Neurology (EXC 2145 SyNergy – ID 390857198) and under the grants LI-2534/6-1, LI-2534/7-1 and LL-112/1-1.

DISCLOSURES

The authors have no competing interests to disclose.

REFERENCES:

1 Collaborators, G. B. D. C. o. D. Global, regional, and national age-sex specific mortality for 264 causes of death, 1980-2016: a systematic analysis for the Global Burden of Disease Study 2016. *Lancet.* **390** (10100), 1151-1210, doi:10.1016/S0140-6736(17)32152-9, (2017).

2 Carmichael, S. T. Rodent models of focal stroke: size, mechanism, and purpose. *NeuroRx.* **2** (3), 396-409, doi:10.1602/neurorx.2.3.396, (2005).

3 Rosenblum, W. I. & El-Sabban, F. Platelet aggregation in the cerebral microcirculation: effect of aspirin and other agents. *Circ Res.* **40** (3), 320-328, doi:10.1161/01.res.40.3.320, (1977).

4 Watson, B. D., Dietrich, W. D., Busto, R., Wachtel, M. S. & Ginsberg, M. D. Induction of reproducible brain infarction by photochemically initiated thrombosis. *Ann Neurol.* **17** (5), 497-504, doi:10.1002/ana.410170513, (1985).

5 Bergeron, M. Inducing photochemical cortical lesions in rat brain. *Curr Protoc Neurosci.* **Chapter 9** Unit 9 16, doi:10.1002/0471142301.ns0916s23, (2003).

6 Lee, J. K. *et al.* Photochemically induced cerebral ischemia in a mouse model. *Surg Neurol.* **67** (6), 620-625; discussion 625, doi:10.1016/j.surneu.2006.08.077, (2007).

7 Dietrich, W. D., Watson, B. D., Busto, R., Ginsberg, M. D. & Bethea, J. R. Photochemically induced cerebral infarction. I. Early microvascular alterations. *Acta Neuropathol.* **72** (4), 315-325, doi:10.1007/BF00687262, (1987).

8 McNutt, M. Journals unite for reproducibility. *Science.* **346** (6210), 679, doi:10.1126/science.aaa1724, (2014).

9 Llovera, G. *et al.* Results of a preclinical randomized controlled multicenter trial (pRCT): Anti-CD49d treatment for acute brain ischemia. *Sci Transl Med.* **7** (299), 299ra121, doi:10.1126/scitranslmed.aaa9853, (2015).

10 Dirnagl, U. *et al.* A concerted appeal for international cooperation in preclinical stroke research. *Stroke.* **44** (6), 1754-1760, doi:10.1161/STROKEAHA.113.000734, (2013).

11 Bath, P. M., Macleod, M. R. & Green, A. R. Emulating multicentre clinical stroke trials: a new paradigm for studying novel interventions in experimental models of stroke. *Int J Stroke.* **4** (6), 471-479, doi:10.1111/j.1747-4949.2009.00386.x, (2009).

12 Kilkenny, C., Browne, W. J., Cuthill, I. C., Emerson, M. & Altman, D. G. Improving bioscience research reporting: The ARRIVE guidelines for reporting animal research. *J Pharmacol Pharmacother.* **1** (2), 94-99, doi:10.4103/0976-500X.72351, (2010).

13 Llovera, G. & Liesz, A. The next step in translational research: lessons learned from the first preclinical randomized controlled trial. *J Neurochem.* **139 Suppl 2** 271-279, doi:10.1111/jnc.13516, (2016).

14 Gnyawali, S. C. *et al.* Retooling Laser Speckle Contrast Analysis Algorithm to Enhance Non-Invasive High Resolution Laser Speckle Functional Imaging of Cutaneous Microcirculation. *Sci Rep.* **7** 41048, doi:10.1038/srep41048, (2017).

15 Clark, W. M., Lessov, N. S., Dixon, M. P. & Eckenstein, F. Monofilament intraluminal middle cerebral artery occlusion in the mouse. *Neurol Res.* **19** (6), 641-648, doi:10.1080/01616412.1997.11740874, (1997).

16 Swanson, G. M., Satariano, E. R., Satariano, W. A. & Threatt, B. A. Racial differences in the early detection of breast cancer in metropolitan Detroit, 1978 to 1987. *Cancer.* **66** (6), 1297-1301 (1990).

17 Longa, E. Z., Weinstein, P. R., Carlson, S. & Cummins, R. Reversible middle cerebral artery occlusion without craniectomy in rats. *Stroke.* **20** (1), 84-91, doi:10.1161/01.str.20.1.84, (1989).
18 Engel, O., Kolodziej, S., Dirnagl, U. & Prinz, V. Modeling stroke in mice - middle cerebral artery occlusion with the filament model. *J Vis Exp.* (47), doi:10.3791/2423, (2011).
19 Tamura, A., Graham, D. I., McCulloch, J. & Teasdale, G. M. Focal cerebral ischaemia in the rat: 1. Description of technique and early neuropathological consequences following middle cerebral artery occlusion. *J Cereb Blood Flow Metab.* **1** (1), 53-60, doi:10.1038/jcbfm.1981.6, (1981).
20 Chen, S. T., Hsu, C. Y., Hogan, E. L., Maricq, H. & Balentine, J. D. A model of focal ischemic stroke in the rat: reproducible extensive cortical infarction. *Stroke.* **17** (4), 738-743 (1986).
21 Tureyen, K., Vemuganti, R., Sailor, K. A. & Dempsey, R. J. Infarct volume quantification in mouse focal cerebral ischemia: a comparison of triphenyltetrazolium chloride and cresyl violet staining techniques. *J Neurosci Methods.* **139** (2), 203-207, doi:10.1016/j.jneumeth.2004.04.029, (2004).
22 Llovera, G., Roth, S., Plesnila, N., Veltkamp, R. & Liesz, A. Modeling stroke in mice: permanent coagulation of the distal middle cerebral artery. *J Vis Exp.* (89), e51729, doi:10.3791/51729, (2014).
23 Cramer, J. V. *et al.* In vivo widefield calcium imaging of the mouse cortex for analysis of network connectivity in health and brain disease. *Neuroimage.* **199** 570-584, doi:10.1016/j.neuroimage.2019.06.014, (2019).
24 Heindl, S. *et al.* Automated Morphological Analysis of Microglia After Stroke. *Front Cell Neurosci.* **12** 106, doi:10.3389/fncel.2018.00106, (2018).
25 Nih, L. R., Gojgini, S., Carmichael, S. T. & Segura, T. Dual-function injectable angiogenic biomaterial for the repair of brain tissue following stroke. *Nat Mater.* **17** (7), 642-651, doi:10.1038/s41563-018-0083-8, (2018).
26 Rust, R. *et al.* Nogo-A targeted therapy promotes vascular repair and functional recovery following stroke. *Proc Natl Acad Sci U S A.* **116** (28), 14270-14279, doi:10.1073/pnas.1905309116, (2019).
27 Kitano, H., Kirsch, J. R., Hurn, P. D. & Murphy, S. J. Inhalational anesthetics as neuroprotectants or chemical preconditioning agents in ischemic brain. *J Cereb Blood Flow Metab.* **27** (6), 1108-1128, doi:10.1038/sj.jcbfm.9600410, (2007).
28 Farr, T. D. & Whishaw, I. Q. Quantitative and qualitative impairments in skilled reaching in the mouse (Mus musculus) after a focal motor cortex stroke. *Stroke.* **33** (7), 1869-1875, doi:10.1161/01.str.0000020714.48349.4e, (2002).
29 Kassem-Moussa, H. & Graffagnino, C. Nonocclusion and spontaneous recanalization rates in acute ischemic stroke: a review of cerebral angiography studies. *Arch Neurol.* **59** (12), 1870-1873 (2002).
30 Labat-gest, V. & Tomasi, S. Photothrombotic ischemia: a minimally invasive and reproducible photochemical cortical lesion model for mouse stroke studies. *J Vis Exp.* (76), doi:10.3791/50370, (2013).
31 Sigler, A., Goroshkov, A. & Murphy, T. H. Hardware and methodology for targeting single brain arterioles for photothrombotic stroke on an upright microscope. *J Neurosci Methods.* **170** (1), 35-44, doi:10.1016/j.jneumeth.2007.12.015, (2008).

Table1: General Neuroscore

	Time-point of scoring		*score*
General Neuroscore	**Hair**	0. Hair neat and clean	
		1. Localized piloerection and dirty hair in 2 body parts (nose and eyes)	
		2. Piloerection and dirty hair in >2body parts	
	Ears (mouse on an open bench top)	0. Normal (ears are stretched laterally and behind, they react by straightening up following noise)	
		1. Stretched laterally but not behind (one or both), they react to noise	
		2. Same as 1. NO Reaction to noise.	
	Eyes (mouse on OBT)	0. Open, clean and quickly follow the surrounding environment	
		1. Open and characterized by aqueous mucus. Slowly follow the surrounding environment	
		2. Open and characterized by dark mucus	
		3. Ellipsoidal shaped and characterized by dark mucus	
		4. Closed	
	Posture (place the mouse on the palm and swing gently)	0. The mouse stands in the upright position with the back parallel to the palm. During swing, it stands rapidly.	
		1. The mouse stands humpbacked. During the swing, it flattens the body to gain stability.	
		2. The head or part of the trunk lies on the palm	
		3. The mouse lies on one side, barely able to recover the upright position.	
		4. The mouse lies in a prone position, not able to recover the upright position.	
	Spontaneos activity (mouse on OBT)	0.The mouse is alert and explores actively	
		1.The mouse seems alert, but it is calm and sluggish	
		2.The mouse explores intermittently and sluggishly	
		3.The mouse is somnolent and numb, few movements on-the-spot	
		4.No spontaneous movements	
	Total score for general scoring (normal=0 max=18)		

Table2: Focal Neuroscore

	Time-point of scoring		*score*
Focal Neuroscore	**Body symmetry** (mouse on OBT, observe the nose-tail line)	0. Normal (Body: normal posture, trunk elevated from the bench, with fore and hindlimbs leaning beneath the body. Tail: straight)	
		1. Slight asymmetry (Body: leans on one side with fore and hindlimbs leaning beneath the body. Tail: slightly bent.)	
		2. Moderate asymmetry (Body: leans on one side with fore and hindlimbs stretched out. Tail: slightly bent).	
		3. Prominent asymmetry (Body: bent, on one side lies on the OBT. Tail: bent)	
		4. Extreme asymmetry (Body: highly bent, on one side constantly lies on the OBT. Tail: highly bent)	
	Gait (mouse on OBT. Observed undisturbed)	0. Normal (gait is flexible, symmetric and quick)	
		1. Stiff, inflexible (humpbacked walk, slower than normal mouse)	
		2. Limping, with asymmetric movements	
		3. Trembling, drifting, falling	
		4. Does not walk spontaneously (when stimulated by gently pushing the mouse walks no longer than 3 steps)	
	Climbing (mouse on a 45° surface. Place the mouse in the center of the gripping surface)	0. Normal (mouse climbs quickly)	
		1. Climbs with strain, limb weakness present.	
		2. Holds onto slope, does not slip or climb	
		3. Slides down slope, unsuccessful effort to prevent fail	
		4. Slides immediately, no effort to prevent fail.	
	Circling behavior (mouse on OBT, free observation)	0. Absent circling behavior	
		1. Predominantly one-side turns.	
		2. Circles to one side, although not constantly.	
		3. Circles constantly to one side.	
		4. Pivoting, swaying, or no movement.	
	Forelimb symmetry (mouse suspended by tail)	0. Normal	
		1. Light asymmetry: mild flexion of contralateral forelimb.	
		2. Marked asymmetry: marked flexion of contralateral limb, the body slightly bends on the ipsilateral side.	
		3. Prominent asymmetry: contralateral forelimb adheres to the trunk.	
		4. Slight asymmetry, no body/limb movement.	
	Compulsory circling (forelimbs on bench, hindlimbs suspended by the tail: it reveals the presence of the contralateral limb palsy)	0. Absent. Normal extension of both forelimbs.	
		1. Tendency to turn to one side (the mouse extends both forelimbs, but starts to turn preferably to one side)	
		2. Circles to one side (the mouse turns towards one side with a slower movement compared to healthy mice)	
		3. Pivots to one side sluggishly (the mouse turns towards one side failing to perform a complete circle)	
		4. Does not advance (the front part of the trunk lies on the bench, slow and brief movements)	
	Whisker response (mouse on the OBT)	0. Normal	
		1. Light asymmetry (the mouse withdraws slowly when stimulated on the contralateral side)	
		2. Prominent asymmetry (no response when stimulated to the contralateral side)	
		3. Absent response contralaterally, slow response when stimulated ipsilaterally.	
		4. Absent response bilaterally	
	Total score for focal deficits (normal=0 max=28)		

Figure 1: Phototrombosis

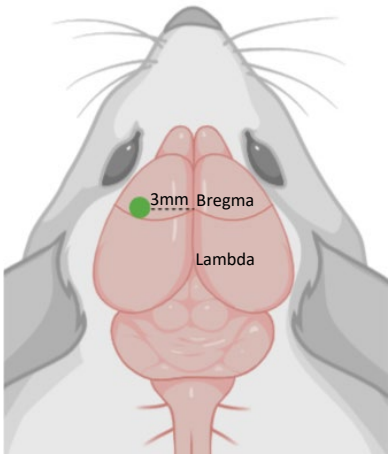

Figure 2: Volumetric infarct analysis and infarct outcome 24h after PT

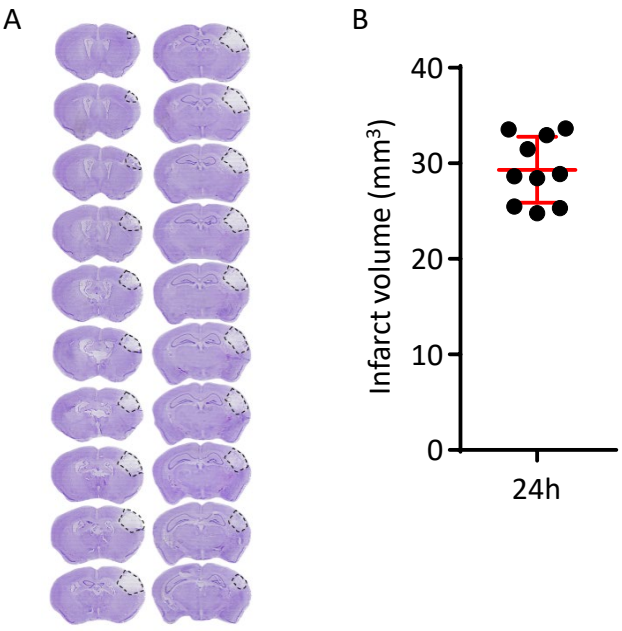

Figure 3: Neuroscore for functional deficits after PT

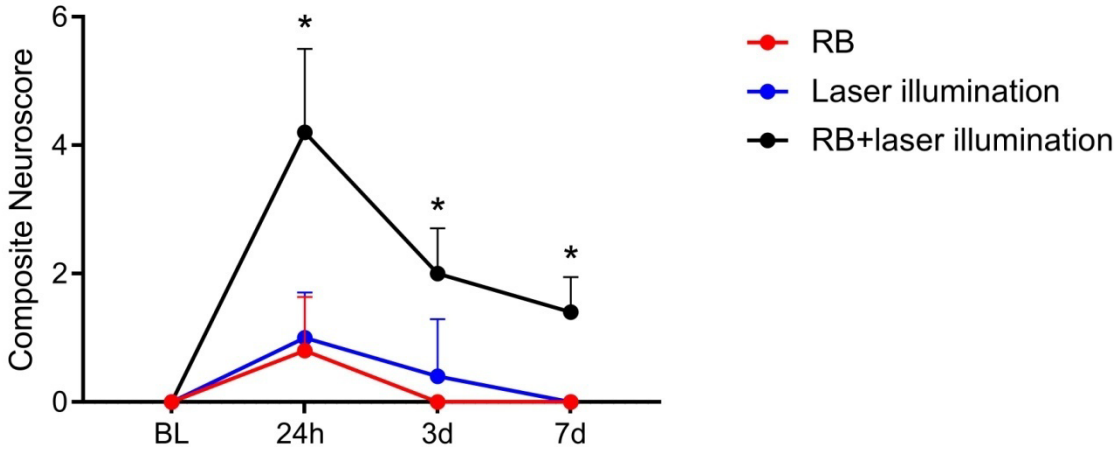

Figure 4: Body weight and temperature analysis 24h after PT

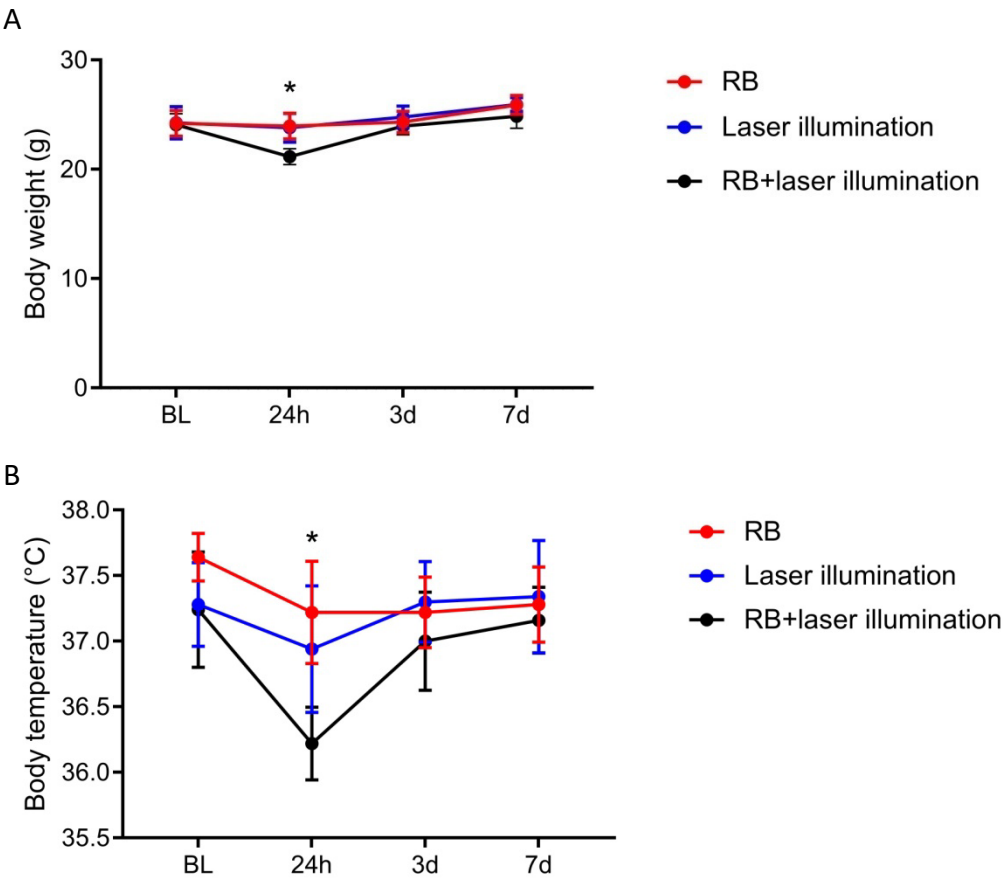

Figure 5: Macroscopic brain evaluation 24h after PT

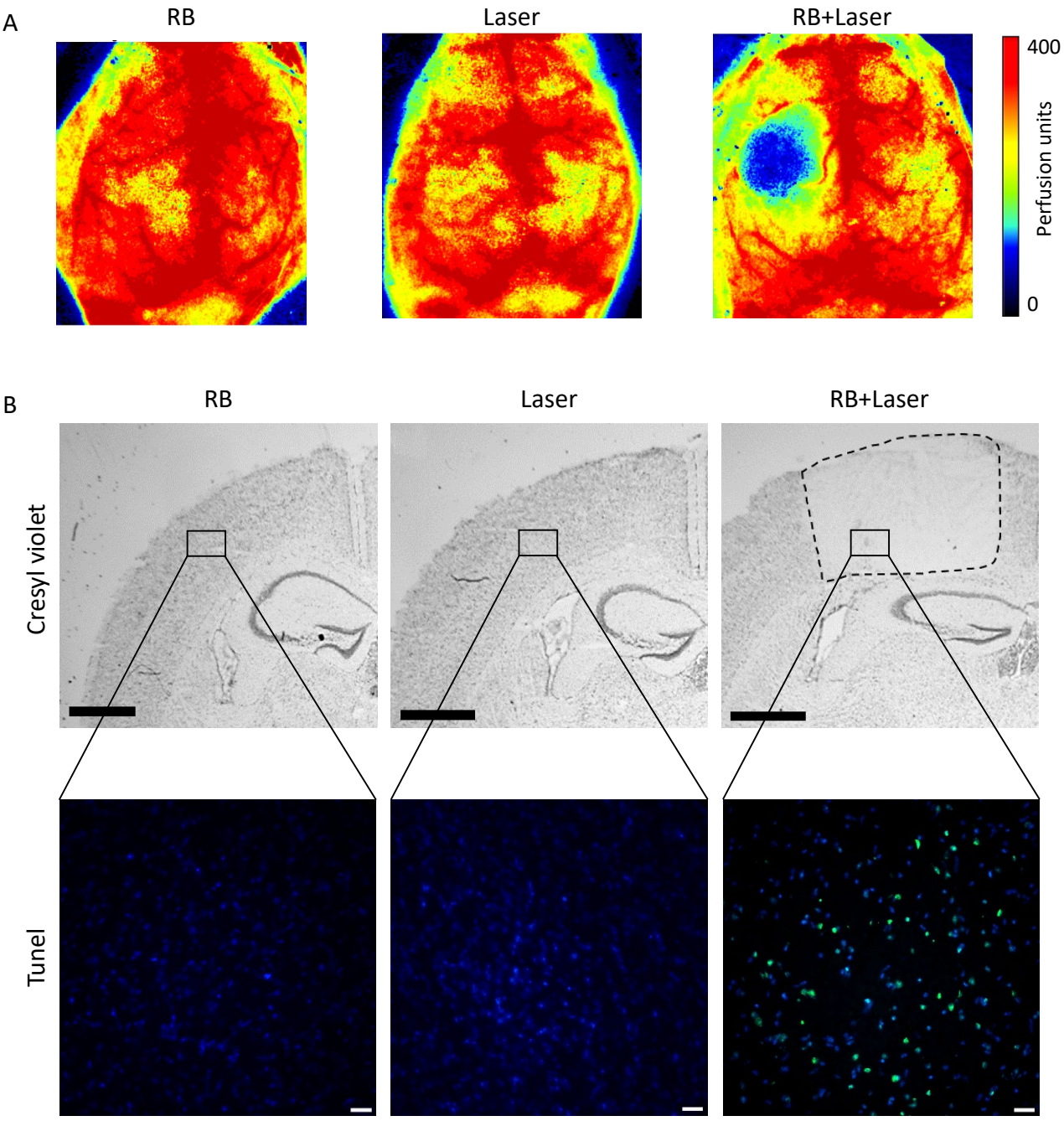

Name of Material/ Equipment	Company	Catalog Number	Comments/Description
561nm wavelenght laser	Solna	Cobolt HS-03	
Acetic Acid	Sigma Life Science	695092	
Anesthesia system for isoflurane	Drager		
ApopTag® Peroxidase In Situ Apoptosis Detection Kit	Millipore	S7100	
Bepanthen pomade	Bayer	1578681	
C57Bl/6J mice	Charles River	000664	
Collimeter	Thorlabs	F240APC-A	
Cotons	NOBA Verbondmitel Danz	974116	
Cresyl violet	Sigma Life Science	C5042-10G	
Cryostat	Thermo Scientific CryoStarNX70		
Ethanol 70%	CLN Chemikalien Laborbedorf	521005	
Ethanol 96%	CLN Chemikalien Laborbedorf	522078	
Ethanol 99%	CLN Chemikalien Laborbedorf	ETO-5000-99-1	
Filter paper	Macherey-Nagel	432018	
Fine Scissors	FST	15000-00	
Forceps	FST	11616-15	
Heating blanket	FHC DC Temperature Controller	40-90-8D	
Isoflurane	Abbot	B506	
Isopentane	Fluka	59070	
Ketamine	Inresa Arzneimittel GmbH		
Laser Speckle	Perimed	PeriCam PSI HR	
Mayor Scissors	FST	1410-15	
Phosphate Buffered Saline PH: 7,4	Apotheke Innestadt Uni Munchen	P32799	
Protective glasses	Laser 2000	NIR-ZS2-38	
Rose Bengal	Sigma Aldrich	198250-5G	
Roti-Histokit mounting medium	Roth	6638.1	
Saline solution	Braun	131321	
Stereomikroskop	Zeiss	Stemi DV4	
Stereotactic frame	Stoelting	51500U	
Superfrost Plus Slides	Thermo Scientific	J1800AMNZ	
Xylacine	Albrecht		